

---

# A Unified Manifold Framework for Modeling Chinese Script Evolution with Application to Oracle Bone Decipherment

---

Tianhao Fu<sup>\*1,2</sup> Xinxin Xu<sup>\*1</sup> Spike Wang<sup>2</sup>

## Abstract

Of the approximately 4,500 Oracle Bone Inscription (OBI) characters discovered from the Shang dynasty, only about 1,600 have been deciphered. Existing computational methods mainly compute the similarity between OBI and single historical period characters independently. However, during the evolution of Chinese characters, significant structural or semantic changes often occur in uncertain dynasties. Relying solely on a single dynasty for reference leads to numerous deciphering errors. Therefore, we propose the **Manifold-based Script Evolution Framework (MSEF)**, the first unified framework that models the evolution series (OBI, Bronze, Seal, Clerical, Regular) of Chinese characters as the continual evolution of a manifold space. MSEF represents each character as an era-specific manifold point and learns continuous inter-era transition rules via Neural Ordinary Differential Equations. Both manifold space and transition dynamics can be trained end-to-end through character evolution pairs across any two eras. To support this training scheme, we construct the first unified cross-era dataset with **fine-grained temporal and regional granularity**. Based on MSEF, we propose the **Cascaded Bidirectional evolutionary Decipherment (CBED)** algorithm, where forward predictions recall potential candidates and backward consistency checking filters false matches—effectively avoiding errors caused by single-dynasty comparisons. Experiments on three commonly used benchmarks and our dataset demonstrate that MSEF achieves state-of-the-art performance among all current oracle deciphering algorithms. Dataset and code are released through our project page.

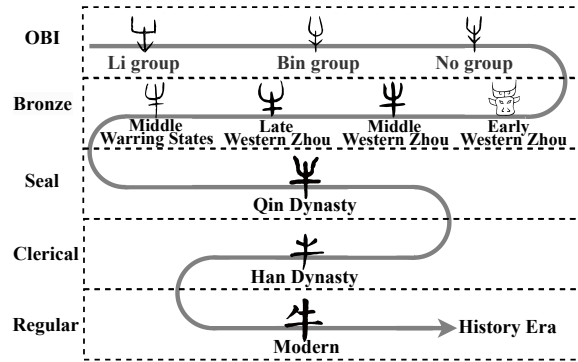


**Figure 1. Evolution of Chinese Script.** Taking the character “Ox” as an illustrative example, this figure demonstrates the evolution of Chinese characters across five historical periods. This character underwent a significant morphological change in early bronze script, then later reverted to a form similar to its oracle bone appearance. Conventional retrieval methods based solely on bronze script would incorrectly judge the similarity as low, leading to decipherment errors. Accurate decipherment requires considering the character’s evolution across multiple dynasties and their temporal dependencies.

## 1. Introduction

Oracle Bone Inscription (OBI) is a cornerstone in the annals of linguistic history, predating many established writing systems (Gil, 2020). Chinese characters evolve over three millennia from Shang dynasty OBI, through Zhou dynasty Bronze Inscriptions, Qin dynasty Seal Script, Han dynasty Clerical Script, to modern Regular Script; figure 1 illustrates the evolution process. Among the approximately 4,500 OBI characters discovered, only about 1,600 (35.6%) have been deciphered (Keightley, 1985; Li et al., 2020). Deciphering the remaining ~2,900 characters would unlock invaluable insights into early Chinese civilization (Wang & Deng, 2024), yet this process often takes years per character due to the need to thoroughly examine structural features and semantic patterns across different eras.

The emergence of AI technologies presents a novel frontier for OBI deciphering. Current approaches generally fall into two categories: (1) compare OBI with modern simplified Chinese by image retrieval (Meng et al., 2018; Hu et al.,

<sup>1</sup>Peking University <sup>2</sup>Fulcrum.AI. Correspondence to: Tianhao Fu <tianhaofu1@gmail.com>.

2024) or generate modern simplified Chinese (Chang et al., 2022; Li et al., 2023c), sometimes incorporating semantic information (Chen et al., 2024); and (2) compare OBI with other historical scripts such as Bronze (Wu et al., 2025b).

The first type attempts direct mappings from OBI-to-modern, ignoring critical intermediate stages (Guo et al., 2015; Zhang et al., 2019; Li et al., 2023b). This proves to be ineffective for characters that underwent major transformations during specific dynasties. The second type, while incorporating multi-era comparisons, treats historical scripts as independent static sets. For instance, CrossFont (Wu et al., 2025b) processes multi-era data but fails to model temporal evolutionary dynamics explicitly, which often leads to making it difficult to recall fonts that underwent drastic changes during the dynasties being compared. Moreover, character lifespans vary significantly—certain OBI glyphs became extinct before the Bronze era—yet approaches that force comparisons across all periods inevitably introduce noise. The current approach does not solve this issue either, but instead proceeds with decipherment under the assumption that all oracle bone inscriptions have survived to the present day. In such a situation, it is crucial to develop a method that fully accounts for the evolutionary patterns of the oracle bone script and considers decipherment across all dynasties. So we propose the **Manifold-based Script Evolution Framework (MSEF)** (Bottéro, 1996; Meilä & Zhang, 2024), modeling character evolution as continuous flow through a shared manifold space directly. Specifically, (1) Under MSEF, Each historical period defines a distinct high-dimensional coordinate system where each character corresponds to a unique point. Inter-period transitions are governed by continuous, invertible Neural Ordinary Differential Equations (Neural ODE) (Chen et al., 2018; Rubanova et al., 2019). (2) We implement the manifold using a time-conditioned transformer mapping feature vectors to coordinates, with a spectrally-normalized network for the ODE ensuring continuous transitions. (3) Furthermore, We additionally introduce a survival network that predicts character extinction probability across dynasties.

To support MSEF training, we **construct a fine-grained dataset** containing 1,500 complete evolution chains and  $\sim 13,700$  pairwise combinations. Based on trained MSEF, we propose **Cascaded Bidirectional Evolutionary Decipherment (CBED)**, which performs forward cascade retrieval with a survival mechanism to terminate extinct paths, followed by backward verification via inverse ODE flows with step-wise pruning for evolutionary consistency.

Our contributions are:

- We propose a Manifold-based Script Evolution Framework (MSEF) which could model the evolution series(OBI, Bronze, Seal, Clerical, Regular) of Chinese characters as the continual evolution of a manifold space.

Such framework contains a manifold net for representing the period, neural ode for representing the period transition, and survival net for representing the Discontinuity of Chinese Characters.

- We construct and opensource the first unified cross-era oracle dataset which could support training the MSEF.
- We introduce a Cascaded Bidirectional Evolutionary Decipherment (CBED) mechanism that employs forward cascaded retrieval with backward verification, providing temporal consistency validation. Such a mechanism could fully leverage the potential of MSEF chinese character evolution knowledge in deciphering oracle bone task.
- Experiments on both 3 Commonly used datasets and our own datasets demonstrate that MSEF achieves the state-of-the-art among all currnet oracle deciphering algorithms.

## 2. Related Work

Our work relates to two research directions: manifold learning for temporal data and computational OBI analysis.

### 2.1. Manifold Learning for Temporal Data

Manifold learning (Izenman, 2012) assumes high-dimensional data lies on lower-dimensional manifolds. Neural ODEs (Biloš et al., 2021; Dupont et al., 2019) extended this to continuous-time dynamical systems, enabling applications in video generation and time series analysis (Shnitzer et al., 2016). Normalizing flows on manifolds further enabled density estimation on non-Euclidean spaces (Kim et al., 2020).

### 2.2. Computational OBI Analysis

Existing computational OBI methods are either direct OBI-to-modern mapping or pairwise cross-era comparison, which ignore the rich intermediate stages. The former includes generative approaches such as OracleFusion (Li et al., 2025b), dual conditional diffusion models (Wu et al., 2025a), and Diff-Oracle (Guan et al., 2024), as well as component-level segmentation methods (Hu et al., 2025). With the rise of Large Multimodal Models, recent benchmarks such as OracleAgent (Li et al., 2025a), OBI-Bench (Chen et al., 2024), and OracleSage (Jiang et al., 2024) focus on aligning visual OBI features directly with modern semantic knowledge. Although CrossFont (Wu et al., 2025b) uses a CrossFont image retrieval network to leverage data from other historical periods, it lacks a unified framework to enforce temporal consistency across the entire evolutionary chain, which is a crucial step in deciphering for traditional archeology experts.

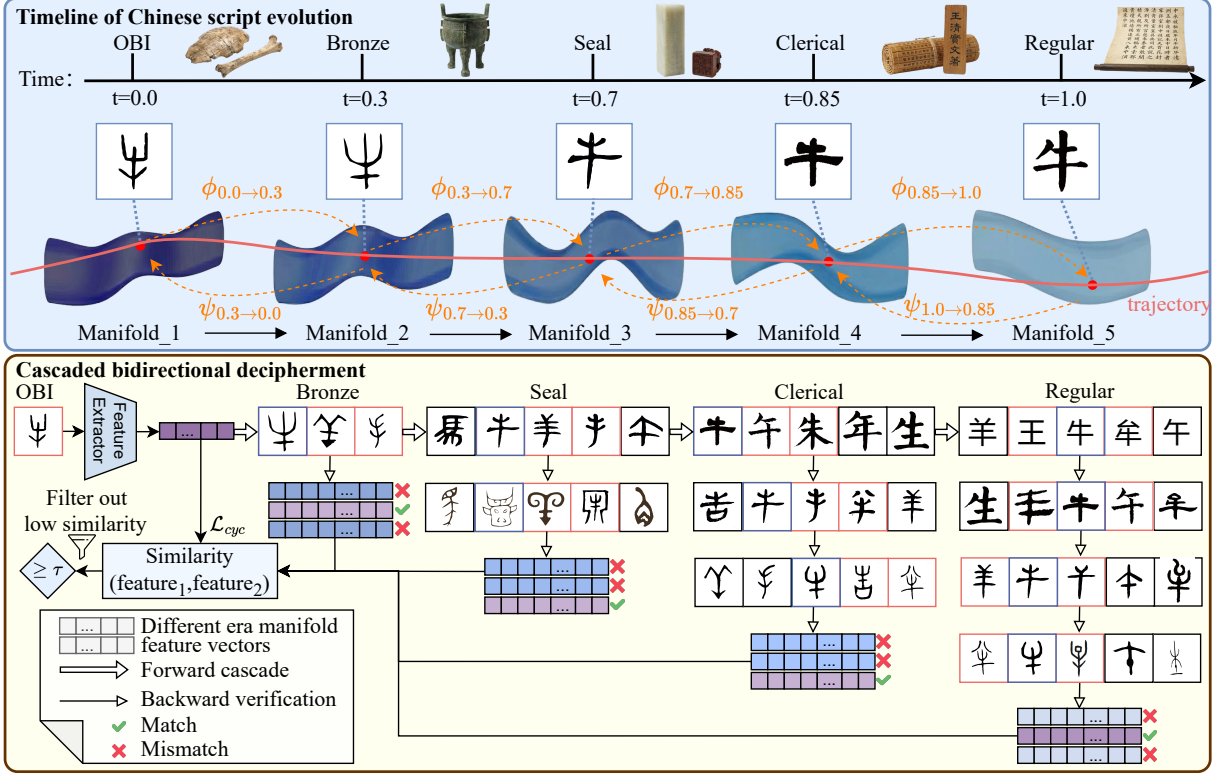


**Figure 2. Overview of MSEF. Top: Continuous Manifold Evolution.** The framework models the 3,000-year evolution of Chinese script as a continuous trajectory (red line) through era-specific manifolds  $\mathcal{M}_t$ , conditioned on normalized time  $t$  (from OBI  $t = 0.0$  to Regular  $t = 1.0$ ). Neural ODEs govern the continuous transitions via forward flows  $\phi$  and backward flows  $\psi$ . Specifically, Each historical period manifold defines a distinct high-dimensional coordinate system where each character corresponds to a unique point. Inter-period point transitions are governed by the continuous neural ODE. Such a framework enables us to derive candidate character solutions for any dynasty within the character manifold space by leveraging any given dynasty. This facilitates the design of subsequent bidirectional cascading decryption algorithms. **Bottom: Cascaded Bidirectional Decipherment.** The inference process consists of two stages: (1) **Forward Recall:** Given an OBI query, the model progressively infers its coordinate in subsequent eras (Bronze  $\rightarrow$  Seal  $\rightarrow$  Clerical  $\rightarrow$  Regular) to retrieve candidate sets. (2) **Backward Verification:** Candidates from the modern era are traced back through history via inverse flows. At each reverse transition, candidates showing large reconstruction errors (marked with  $\times$ ) are pruned step-by-step. The final decipherment is determined by the cycle consistency similarity with the original OBI features (filtered by threshold  $\tau$ ).

### 3. Manifold-based Script Evolution Framework (MSEF)

In this section, we describe the proposed MSEF and corresponding CBED. We first present our observation and intuition of the Chinese character evolution in section 3.1, and then introduce the Theoretical Form of the Evolution of Chinese Characters in section 3.2, which unifies distinct historical eras into a single evolving manifold governed by differential equations. After that we introduce how we implement and train such a mathematical model in Sections 3.4 and 3.4. Finally, By learning the vector field of character evolution, MSEF allows us to project ancient scripts forward to predict their modern counterparts and trace modern characters backward to verify their origins. Such Cascaded Bidirectional evolutionary Decipherment algorithm is illustrated in section 3.5.

#### 3.1. Intuition: Script Evolution as Continuous Flow

Figure 2 visualizes the continuous evolution using “ox” as an example. Tracing the evolution from the OBI to the Regular, we observe that despite drastic stylistic shifts, the character preserves its fundamental topological structure. In such a situation, We must apply temporal modeling to textual evolution to capture these uncertain shifts, thereby enhancing decoding accuracy. To demonstrate more of the case of these uncertain change patterns, Figure 3 presents evolutionary trajectories for a wider set of characters.

We model this dynamic evolution process as a continuous flow through a shared geometric space. All characters are points in a high-dimensional manifold  $\mathcal{M}$ . As time progresses, each point moves along a smooth trajectory governed by learnable dynamics. This allows us to trace any











## Impact Statement

This work advances machine learning for digital humanities by accelerating the decipherment of OBI. Our MSEF framework and the released cross-era dataset aim to preserve cultural heritage and facilitate interdisciplinary research by assisting paleographers in processing large-scale archaeological data.

**Ethical Considerations.** We acknowledge the risk of model misinterpretation. Therefore, MSEF is designed strictly as an *assistive tool* to augment, not replace, expert analysis. We foresee no issues regarding privacy or discrimination, as our data consists of public domain ancient artifacts.

It should be noted that truly deciphering oracle bone inscriptions requires writing a comprehensive and detailed scholarly report that gains recognition within the academic community. Therefore, like other AI-based methods for deciphering oracle bone inscriptions, this approach serves only as an auxiliary tool. Actual deciphering efforts require collaboration with archeologists.

For specific details, please stay tuned for our forthcoming open-source project: a deciphering article co-authored by our AI system and archeology experts.

## References

- The Complete Collection of Ancient and Modern Characters (CCAMC). <http://www.ccamc.co>, 2024. Accessed: 2026-01-28.
- The Amazing Oracle Bone Inscriptions (LBQJQW). <https://www.jgwlbq.org.cn/>, 2024. Accessed: 2026-01-28.
- Beijing Normal University. Beijing Normal University Character Database (BNU). <https://www.bnu.edu.cn/>, 2024. Accessed: 2026-01-28.
- Biloš, M., Sommer, J., Rangapuram, S. S., Januschowski, T., and Günemann, S. Neural flows: Efficient alternative to neural odes. *Advances in neural information processing systems*, 34:21325–21337, 2021.
- Bottéro, F. The origin and early development of the chinese writing system, 1996.
- Chang, X., Chao, F., Shang, C., and Shen, Q. Sundial-gan: A cascade generative adversarial networks framework for deciphering oracle bone inscriptions. In *Proceedings of the 30th ACM international conference on multimedia*, pp. 1195–1203, 2022.
- Chen, R. T., Rubanova, Y., Bettencourt, J., and Duvenaud, D. K. Neural ordinary differential equations. *Advances in neural information processing systems*, 31, 2018.
- Chen, Z., Chen, T., Zhang, W., and Zhai, G. Obi-bench: Can Imms aid in study of ancient script on oracle bones? *arXiv preprint arXiv:2412.01175*, 2024.
- Chen, Z., Hua, W., Li, J., Deng, L., Du, F., Chen, T., and Zhai, G. Pictobi-20k: Unveiling large multimodal models in visual decipherment for pictographic oracle bone characters. *arXiv preprint arXiv:2509.05773*, 2025.
- Dupont, E., Doucet, A., and Teh, Y. W. Augmented neural odes. *Advances in neural information processing systems*, 32, 2019.
- Gil, J. Will a character based writing system stop chinese becoming a global language? a review and reconsideration of the debate. *Global Chinese*, 6(1):25–48, 2020.
- Guan, H., Yang, H., Wang, X., Han, S., Liu, Y., Jin, L., Bai, X., and Liu, Y. Deciphering oracle bone language with diffusion models. *arXiv preprint arXiv:2406.00684*, 2024.
- Guo, J., Wang, C., Roman-Rangel, E., Chao, H., and Rui, Y. Building hierarchical representations for oracle character and sketch recognition. *IEEE Transactions on Image Processing*, 25(1):104–118, 2015.
- Hu, Z., Cheung, Y.-m., Zhang, Y., Zhang, P., and Tang, P.-l. Component-level oracle bone inscription retrieval. In *Proceedings of the 2024 International Conference on Multimedia Retrieval*, pp. 647–656, 2024.
- Hu, Z., Cheung, Y.-m., Zhang, Y., Peiying, Z., and Ling, T. P. Component-level segmentation for oracle bone inscription decipherment. In *Proceedings of the AAAI Conference on Artificial Intelligence*, volume 39, pp. 28116–28124, 2025.
- Isola, P., Zhu, J.-Y., Zhou, T., and Efros, A. A. Image-to-image translation with conditional adversarial networks. In *Proceedings of the IEEE conference on computer vision and pattern recognition*, pp. 1125–1134, 2017.
- Izenman, A. J. Introduction to manifold learning. *Wiley Interdisciplinary Reviews: Computational Statistics*, 4(5): 439–446, 2012.
- Jiang, H., Pan, Y., Chen, J., Liu, Z., Zhou, Y., Shu, P., Li, Y., Zhao, H., Mihm, S., Howe, L. C., et al. Oraclesage: Towards unified visual-linguistic understanding of oracle bone scripts through cross-modal knowledge fusion. *arXiv preprint arXiv:2411.17837*, 2024.
- Keightley, D. N. *Sources of Shang history: the oracle-bone inscriptions of Bronze Age China*. Univ of California Press, 1985.

- Kim, H., Lee, H., Kang, W. H., Lee, J. Y., and Kim, N. S. Softflow: Probabilistic framework for normalizing flow on manifolds. *Advances in Neural Information Processing Systems*, 33:16388–16397, 2020.
- Lee, H.-Y., Tseng, H.-Y., Huang, J.-B., Singh, M., and Yang, M.-H. Diverse image-to-image translation via disentangled representations. In *Proceedings of the European conference on computer vision (ECCV)*, pp. 35–51, 2018.
- Li, B., Dai, Q., Gao, F., Zhu, W., Li, Q., and Liu, Y. Hwobc—a handwriting oracle bone character recognition database. In *Journal of Physics: Conference Series*, volume 1651, pp. 012050. IOP Publishing, 2020.
- Li, B., Xue, K., Liu, B., and Lai, Y.-K. Bbdm: Image-to-image translation with brownian bridge diffusion models. In *Proceedings of the IEEE/CVF conference on computer vision and pattern Recognition*, pp. 1952–1961, 2023a.
- Li, C., Ding, Z., Hu, X., Li, B., Luo, D., Peng, X., Jin, T., Liu, Y., Han, S., Yang, J., et al. Oracleagent: A multimodal reasoning agent for oracle bone script research. *arXiv preprint arXiv:2510.26114*, 2025a.
- Li, C., Ding, Z., Hu, X., Li, B., Luo, D., Wu, A., Wang, C., Wang, C., Jin, T., Shu, S., et al. Oraclefusion: Assisting the decipherment of oracle bone script with structurally constrained semantic typography. In *Proceedings of the IEEE/CVF International Conference on Computer Vision*, pp. 19893–19902, 2025b.
- Li, J., Wang, Q.-F., Huang, K., Yang, X., Zhang, R., and Goulermas, J. Y. Towards better long-tailed oracle character recognition with adversarial data augmentation. *Pattern Recognition*, 140:109534, 2023b.
- Li, J., Wang, Q.-F., Wang, S., Zhang, R., Huang, K., and Cambria, E. Diff-oracle: Deciphering oracle bone scripts with controllable diffusion model. *arXiv preprint arXiv:2312.13631*, 2023c.
- Loshchilov, I. and Hutter, F. Decoupled weight decay regularization. *arXiv preprint arXiv:1711.05101*, 2017.
- Meilă, M. and Zhang, H. Manifold learning: What, how, and why. *Annual Review of Statistics and Its Application*, 11(1):393–417, 2024.
- Meng, L., Kamitoku, N., and Yamazaki, K. Recognition of oracle bone inscriptions using deep learning based on data augmentation. In *2018 metrology for archaeology and cultural heritage (MetroArchaeo)*, pp. 33–38. IEEE, 2018.
- Rubanova, Y., Chen, R. T., and Duvenaud, D. K. Latent ordinary differential equations for irregularly-sampled time series. *Advances in neural information processing systems*, 32, 2019.
- Saharia, C., Chan, W., Chang, H., Lee, C., Ho, J., Salimans, T., Fleet, D., and Norouzi, M. Palette: Image-to-image diffusion models. In *ACM SIGGRAPH 2022 conference proceedings*, pp. 1–10, 2022a.
- Saharia, C., Ho, J., Chan, W., Salimans, T., Fleet, D. J., and Norouzi, M. Image super-resolution via iterative refinement. *IEEE transactions on pattern analysis and machine intelligence*, 45(4):4713–4726, 2022b.
- Seo, M., Baek, J., Lee, S., and Hwang, S. J. Paper2code: Automating code generation from scientific papers in machine learning. *arXiv preprint arXiv:2504.17192*, 2025.
- Shnitzer, T., Talmon, R., and Slotine, J.-J. Manifold learning with contracting observers for data-driven time-series analysis. *IEEE Transactions on Signal Processing*, 65(4):904–918, 2016.
- Wang, M. and Deng, W. A dataset of oracle characters for benchmarking machine learning algorithms. *Scientific Data*, 11(1):87, 2024.
- Wu, R., Wang, S., Li, X., and Liu, D. A text image dual conditional stable diffusion model for oracle bone inscription decipherment. *npj Heritage Science*, 13(1):453, 2025a.
- Wu, Z., Su, Q., Gu, K., and Shi, X. A cross-font image retrieval network for recognizing undeciphered oracle bone inscriptions. In *International Conference on Intelligent Computing*, pp. 196–208. Springer, 2025b.
- Zhang, Y.-K., Zhang, H., Liu, Y.-G., Yang, Q., and Liu, C.-L. Oracle character recognition by nearest neighbor classification with deep metric learning. In *2019 International Conference on Document Analysis and Recognition (ICDAR)*, pp. 309–314. IEEE, 2019.
- Zhu, J.-Y., Park, T., Isola, P., and Efros, A. A. Unpaired image-to-image translation using cycle-consistent adversarial networks. In *Proceedings of the IEEE international conference on computer vision*, pp. 2223–2232, 2017.









where  $E(0)$  is the initial encoding error at  $t = 0$ .

*Proof.* The evolution is governed by the ODE  $\frac{dz}{dt} = v(z, t)$ . The error rate of change is:

$$\begin{aligned} \frac{d}{dt}E(t) &= \frac{d}{dt}\|\hat{z}(t) - z^*(t)\| \\ &\leq \|\hat{v}(\hat{z}, t) - v^*(z^*, t)\| \\ &\leq \|\hat{v}(\hat{z}, t) - \hat{v}(z^*, t)\| + \|\hat{v}(z^*, t) - v^*(z^*, t)\| \\ &\leq L\|\hat{z}(t) - z^*(t)\| + \epsilon \\ &= LE(t) + \epsilon \end{aligned} \tag{27}$$

Applying Grönwall's Inequality to the differential inequality  $\dot{E}(t) \leq LE(t) + \epsilon$  yields the stated bound.  $\square$

#### Scenario Analysis: Direct vs. Cascaded Inference.

**Scenario 1: Direct Mapping (OBI  $\rightarrow$  Regular).** Predicting the modern form ( $t = 1$ ) directly from OBI ( $t = 0$ ) accumulates error exponentially over  $\Delta t = 1$ :

$$E_{direct} \leq \frac{\epsilon}{L}(e^L - 1) \tag{28}$$

For complex evolution dynamics (large  $L$ ), this bound becomes loose, explaining the low accuracy of direct baselines.

**Scenario 2: Cascaded Inference (MSEF).** By utilizing intermediate eras (Bronze, Seal, Clerical) as checkpoints, we divide the total time into  $K$  smaller intervals  $\Delta t_i$ . The retrieval step at each era  $t_i$  acts as a "re-anchoring" mechanism, effectively resetting the accumulated drift. The multi-step error bound is significantly tighter:

$$E_{cascaded} \approx \sum_{i=0}^{K-1} \frac{\epsilon}{L}(e^{L\Delta t_i} - 1) \tag{29}$$

Since  $e^{L\sum \Delta t_i} \gg \sum e^{L\Delta t_i}$  for convex exponential functions, this proves that breaking the long trajectory into shorter segments strictly reduces the upper bound of the inference error.

#### B.1.7. THEOREM 2: DYNAMIC EVOLUTION OF VARIANT DISTRIBUTIONS

We derive the governing law for how the probability distribution of character variants evolves along the manifold. This provides the theoretical basis for Assumption 3, explaining how the model handles the transition from high-variance OBI forms to standardized Regular scripts.

**Theorem 2 (Instantaneous Change of Variables).** Let  $p(z(t), t)$  denote the probability density of a character state  $z(t)$  at time  $t$ . Given the continuous dynamics  $\frac{dz(t)}{dt} = v(z(t), t)$ , the log-density of the distribution evolves according to the following ordinary differential equation:

$$\frac{d \log p(z(t), t)}{dt} = -\text{Tr} \left( \frac{\partial v(z(t), t)}{\partial z(t)} \right) \tag{30}$$

where  $\text{Tr}(\cdot)$  denotes the trace operator and  $\frac{\partial v}{\partial z}$  is the Jacobian matrix of the velocity field.

*Proof.* Consider the transformation of a variable  $z(t)$  to  $z(t + \epsilon)$  over an infinitesimal time step  $\epsilon$ :

$$z(t + \epsilon) = z(t) + \epsilon v(z(t), t) + O(\epsilon^2) \tag{31}$$

By the change of variables formula, the probability density transforms as:

$$p(z(t + \epsilon), t + \epsilon) = p(z(t), t) \left| \det \frac{\partial z(t)}{\partial z(t + \epsilon)} \right| \tag{32}$$

Taking the logarithm:

$$\log p(z(t + \epsilon), t + \epsilon) = \log p(z(t), t) - \log \left| \det \frac{\partial z(t + \epsilon)}{\partial z(t)} \right| \tag{33}$$





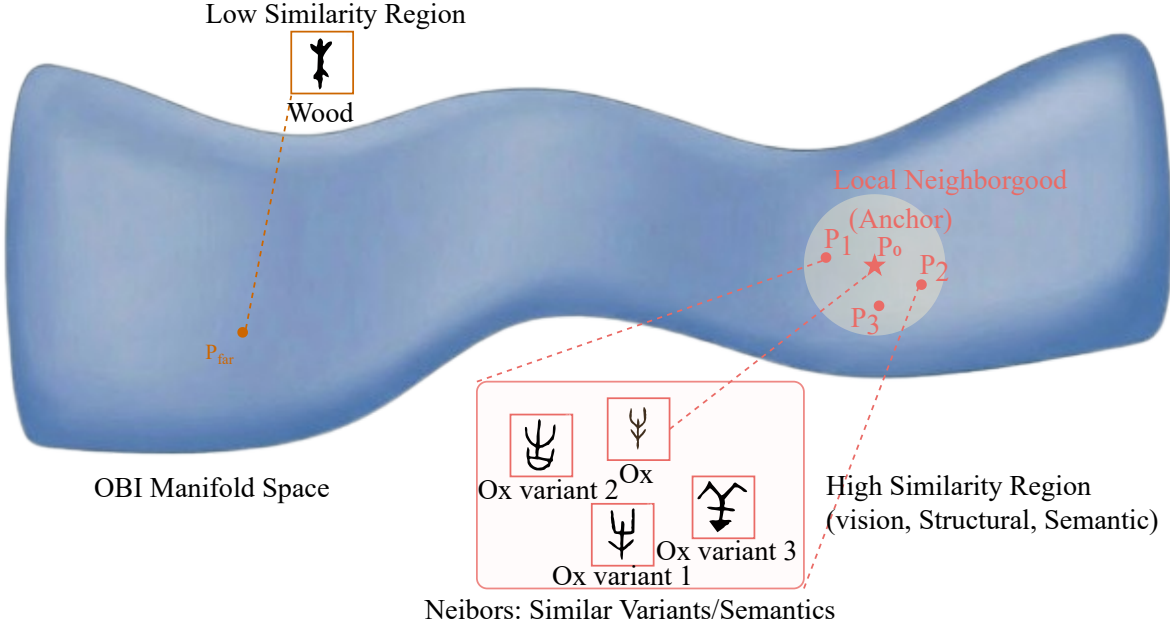


**Figure 4. Manifold visualization by radical groups.** Colors: “口” (red), “水” (blue), “木” (green), “金” (yellow). Shapes: circle (OBI), triangle (Bronze), square (Seal), diamond (Clerical), star (Regular). Gray lines trace evolution trajectories.

- Spring and Autumn:  $t = 0.35\text{--}0.45$
- Warring States:  $t = 0.45\text{--}0.55$

## D. Feature Extraction Details

We extract a 352-dimensional feature vector  $\mathbf{f} \in \mathbb{R}^{352}$  specifically designed for paleographic analysis. The representation aggregates five complementary modalities capturing visual appearance, structural composition, semantic meaning, archaeological context, and spatiotemporal provenance. All features are pre-computed offline before training.

### Visual Features (128-dim):

- Contour descriptors: 32 dimensions (Fourier descriptors, curvature)
- Stroke features: 32 dimensions (stroke count, direction histogram)
- Topological features: 16 dimensions (Euler number, hole count)
- Symmetry measures: 16 dimensions (reflection, rotation)
- Density distribution: 32 dimensions ( $4 \times 4$  grid density, CNN encoding)

### Structural Features (64-dim):

- Formation type: 6 dimensions (one-hot *liushu* encoding)
- Component decomposition: 42 dimensions (radical embeddings)
- Spatial layout: 16 dimensions (left-right, top-bottom, enclosure)

### Semantic Features (64-dim):

- Definition embedding: 64 dimensions (BERT embedding of character meaning from *Shuowen Jiezi* 《说文解字》 and other authoritative dictionaries)

#### Context Features (64-dim):

- Co-occurrence embedding: 64 dimensions (aggregated features of co-occurring characters)

Characters inscribed on the same archaeological artifact (e.g., oracle bone fragment/甲骨片, bronze vessel/青铜器) often share semantic or thematic relationships. We compute the context feature as the mean of the visual, structural, and semantic features of all other characters appearing on the same excavated object:

$$\mathbf{f}_{\text{ctx}}^{(c)} = \frac{1}{|\mathcal{N}(c)|} \sum_{c' \in \mathcal{N}(c)} \left( \mathbf{f}_{\text{vis}}^{(c')} \oplus \mathbf{f}_{\text{str}}^{(c')} \oplus \mathbf{f}_{\text{sem}}^{(c')} \right) \quad (37)$$

where  $\mathcal{N}(c)$  denotes the set of characters co-occurring with character  $c$  on the same artifact, and  $\oplus$  denotes concatenation followed by linear projection to 64 dimensions. This contextual information is particularly valuable for undeciphered OBI, where the surrounding characters may provide crucial semantic clues.

#### Spatiotemporal Features (32-dim):

- Temporal encoding: 16 dimensions (dynasty/period embedding with sinusoidal encoding)
- Spatial encoding: 16 dimensions (latitude and longitude coordinates of excavation site, encoded via positional embedding)

The spatiotemporal features capture provenance information of the excavated artifact, including the historical period (e.g., scribal group for OBI, dynastic sub-period for Bronze) and the geographic location of the excavation site.

**Handling Missing Data.** Due to the fragmentary nature of archeological records, not all characters have complete feature information across all dynasties. When specific data are unavailable for a character in a particular dynasty (e.g., missing co-occurrence information, unknown excavation coordinates, or absent semantic definitions for undeciphered characters), the corresponding feature dimensions are filled with zeros. This zero-padding strategy allows the model to gracefully handle incomplete data while preserving the fixed-dimensional input structure required by the neural network. Note that since we have already incorporated various data-missing scenarios during training, this approach can mitigate the issue of missing data to a certain extent.

## E. Implementation Details

We implement the MSEF framework using PyTorch. All experiments were conducted on a compute node equipped with 8 NVIDIA H100 GPUs. Table 19 provides the complete list of hyperparameters used in our experiments to ensure reproducibility.

**Architecture Configuration.** We set the manifold dimension to  $d = 256$ , which we found to be the optimal trade-off between representational capacity and computational efficiency (see Appendix A.2). The manifold mapping network  $\mathcal{M}_t$  consists of 4 residual blocks with a hidden dimension of 512. The velocity network  $v(z, t)$ , governing the continuous dynamics, is implemented as a 3-layer MLP with 512 hidden units and Tanh activations.

**ODE Integration.** For the neural ODE integration, we utilize the `dopri5` adaptive step-size solver (Dormand-Prince method). We set both relative and absolute tolerances to  $10^{-5}$ . This strict tolerance is crucial for maintaining the reversibility of the flow during the backward verification stage.

**Training Strategy.** The model is optimized using the AdamW optimizer with a learning rate of  $10^{-4}$  and weight decay of  $10^{-4}$ . We employ gradient clipping with a norm threshold of 1.0 to ensure stability during the integration of long trajectories. The training process spans 100 epochs with a batch size of 256.

**Loss Balancing.** The loss weights are empirically tuned to prioritize local continuity while enforcing global consistency. We assign the highest weight ( $\lambda_{adj} = 1.0$ ) to adjacent-era pairs as they provide the most reliable supervision. Cycle consistency ( $\lambda_{cyc} = 0.5$ ) and cross-era constraints ( $\lambda_{skip} = 0.5$ ) act as regularizers to prevent drift over long time horizons.

Table 19. Complete hyperparameter settings for reproducibility.

Hyperparameter	Value
<i>Architecture</i>	
Manifold dimension $d$	256
Feature MLP hidden dim	512
Velocity network layers	3
Velocity network hidden dim	512
ResBlocks count	4
Time embedding dim	64
<i>ODE Solver</i>	
Method	dopri5 (adaptive)
Relative tolerance	$10^{-5}$
Absolute tolerance	$10^{-5}$
<i>Training</i>	
Optimizer	AdamW
Learning rate	$10^{-4}$
Weight decay	$10^{-4}$
Batch size	256
Training epochs	100
Gradient clipping	1.0
<i>Loss Weights</i>	
$\lambda_{\text{adj}}$ (adjacent-era)	1.0
$\lambda_{\text{skip}}$ (cross-era)	0.5
$\lambda_{\text{full}}$ (full-chain)	0.3
$\lambda_{\text{cyc}}$ (cycle consistency)	0.5
$\lambda_{\text{surv}}$ (survival)	0.2
<i>Inference</i>	
Retrieval depth $K$	5
Survival threshold $\tau$	0.1
<i>Hardware</i>	
GPUs	8×NVIDIA H100
Training time	~8 hours

## F. Dataset Construction Details

### Data Sources:

- **LBQJQW** (《了不起的甲骨文》): 154,000+ OBI glyph images with scribal group annotations from the Chinese Academy of Social Sciences.
- **CCAMC** (Chinese Character Ancient Morphology Corpus): 3,772 Bronze characters with period classification from Peking University.
- **BNU** (Beijing Normal University Character Database): 10,516+ characters spanning Seal, Clerical, and Regular scripts with verified correspondences.

To further illustrate the scarcity of deciphered characters and the structural characteristics of the available data, we visualize the data distribution in Figure 5. As shown in the left panel, only approximately 35.6% of the discovered Oracle Bone Inscriptions (OBI) have been deciphered, highlighting the difficulty of the task. The right panel provides a breakdown of the evolutionary chains, demonstrating that while complete chains spanning all five eras are rare (approx. 1,500), there exists a significantly larger volume of partial pairwise correspondences (approx. 13,700). This distribution serves as the primary motivation for constructing a dataset that supports partial chain learning, which is a key feature of our MSEF framework.











Table 29. Computational efficiency comparison.

Method	R@1	Time	Params	GPU
OBSD	41.0*	0.85s	89M	8GB
OracleFusion	58.3	0.95s	89M	8GB
OracleSage	60.1	1.8s	7B	24GB
OracleAgent	62.8	2.3s	7B	28GB
<b>MSEF</b>	<b>72.5</b>	<b>0.18s</b>	<b>140M</b>	<b>6GB</b>

\*OBSD uses generation-based evaluation; R@1 converted from Top-1 accuracy.

## J. Fine-Grained Dataset Visualization

A core contribution of our work is the construction of a dataset with fine-grained temporal and regional annotations, distinct from prior works that rely on single representative glyphs per era.

Figure 8 visualizes 20 representative evolution chains from our dataset. Unlike standard datasets, we preserve intra-era diversity:

- **OBI (Scribal Groups):** We categorize Oracle Bone Inscriptions into eight distinct scribal groups: *Dui* ( $\mathcal{D}$ ), *Bin* ( $\mathcal{B}$ ), *Li* ( $\mathcal{L}$ ), *Chu* ( $\mathcal{C}$ ), *He* ( $\mathcal{H}$ ), *Huang* ( $\mathcal{Hu}$ ), *Zi* ( $\mathcal{Z}$ ), and *None* (indicating unclassified samples). This captures the stylistic variations across different diviner groups and periods within the Shang dynasty.
- **Bronze (Dynastic Sub-periods):** We trace evolution across six specific phases: *Late Shang* (L.S), *Early Western Zhou* (E.Z), *Mid Western Zhou* (M.Z), *Late Western Zhou* (L.Z), *Spring & Autumn* (Sp), and *Warring States* (Wa). Note that for display clarity, sub-stages within Spring & Autumn and Warring States are merged into their respective broader categories.





